ISBN: 978-3-95450-261-5 ISSN: 2673-7000 doi: 10.18429/JACoW-NAPAC2025-TUP053

INSTABILITY THRESHOLD MEASUREMENTS IN THE IOTA RING AT FERMILAB*

M.K. Duncan†, Y.K. Kim[1], University of Chicago, Chicago, IL, USA
R. Ainsworth, N. Eddy, Fermi National Accelerator Laboratory, Batavia, IL, USA
[1]also at Fermi National Accelerator Laboratory, Batavia, IL, USA

Abstract

Nonlinear focusing elements enhance the stability of particle beams in high-energy colliders via Landau Damping, a phenomenon which acts through the tune spread these elements introduce. Our experiment at Fermilab's Integrable Optics Test Accelerator (IOTA) aims to investigate the influence of nonlinear focusing elements on transverse beam stability by using a novel method to directly measure the strength of Landau Damping, employing an active transverse feedback as a controlled source of impedance. The resulting motion of the beam can then be used to directly measure the stability diagram, a threshold that maps the stability conditions of the system. A proof-of-principle experiment of this measurement method was first explored at the LHC, where the experiment at IOTA aims to map out the entirety of the stability diagram and obtain the beam distribution function from the stability diagram, a procedure never done before. Here, we present our simulation results, initial data analysis, and plans for further investigation.

MOTIVATION

A major challenge facing many particle accelerators is maintaining high beam intensity. Factors limiting intensity include collective instabilities, which not only reduce beam intensity but produce losses, irradiate components, and generate other negative effects.

Our group approaches the challenge of intensity by directly studying beam stability at the Integrable Optics Test Accelerator (IOTA) at Fermilab. IOTA is an easily reconfigurable 40 m storage ring designed to run both electrons and protons at energies of 150 MeV and 2.5 MeV, respectively. This experiment is concerned with electrons circulating the ring.

One phenomena studied in understanding beam stability is Landau Damping (LD), which damps collective oscillation modes and acts as a defense against collective instabilities. LD relies on particle betatron frequency spread and works through the energy transfer between coherent and incoherent oscillation modes [1]. Studies on the strength of LD are often approached via Stability Diagram (SD) Theory, which depends on the dispersion relation between the beam's coherent tune shift from an external excitation and the resulting tune of the mode. The dispersion relation for a coherent vertical degree of freedom is shown in Eq. (1):

$$\Delta\omega_y = -1/\int \frac{J_y \partial F/\partial J_y}{\nu - \delta\omega(J_x, J_y) + io}\, dJ_x dJ_y \qquad (1)$$

Where $\Delta\omega_y$ is the coherent tune shift, ν is the tune of the mode, J_y and J_x are the actions in the x and y planes, F is the bunch distribution function, $\delta\omega$ is the oscillating particle frequency shift, and io is a vanishingly small term introduced in derivation to avoid singularities. The distribution function is meant to be normalized: $\int\int F(J_x, J_y) dJ_x dJ_y = 1$ [2].

Given a coherent tune shift, one can use Eq. (1) to find the tune of the mode. To find ν, one would traditionally solve Eq. (1) for all $\Delta\omega$. By mapping $\mathrm{Im}[\nu] = 0$ onto the complex plane of $\Delta\omega$, one obtains a SD, the threshold separating the bunch's stable and unstable states. There currently exist techniques to obtain stability diagrams, although they have limitations as they do not perform direct measurements of SDs [3]. We therefore investigate an alternative method to directly measure stability diagrams. In this method, the polarity of a transverse feedback is reversed, creating an 'antidamper' which excites a coherent mode in the beam, producing a coupling impedance:

$$Z(\omega) \propto Ge^{i\phi}\delta(\omega) \qquad (2)$$

Where G is the gain and ϕ is the phase advance between the pickup and the kick. The $\delta(\omega)$ shows that the antidamper kicks the bunch as a whole. The coupling impedance produces a coherent tune shift:

$$\Delta\omega = ge^{i\phi} \qquad (3)$$

Where g is the growth rate of the beam's centroid position. The gain and phase can be independently changed, making a source of controlled impedance and enabling one to observe at what tune shifts the beam becomes unstable. For the experimental setup at IOTA, the antidamper excitation acts in the y-plane, where the nonlinearity acts in the x-plane. With these conditions, Eq. (1) reduces to:

$$\Delta\omega_y = \left[\int \frac{F_x(J_x)}{\nu - \delta\omega(J_x, J_y) + io} dJ_x\right]^{-1} \qquad (4)$$

With octupoles acting as the source of nonlinearity in the x-plane: $\delta\omega = k\epsilon J_x$, where k is the octupole nonlinearity coefficient and ϵ is the x-plane rms emittance. Our group is working with gaussian beams, where the normalized distribution function is: $F_x(J_x) = e^{-J_x}$. The normalized stability diagram for this distribution is shown in Fig.1. To experimentally obtain Fig.1, G and ϕ are scanned, changing $\Delta\omega$. The top-right subfigure of Fig. 1 shows the beam centroid

* Work supported by the NSF and the Center for Bright Beams
† mbossard@uchicago.edu

ISBN: 978-3-95450-261-5 ISSN: 2673-7000 doi: 10.18429/JACoW-NAPAC2025-TUP053

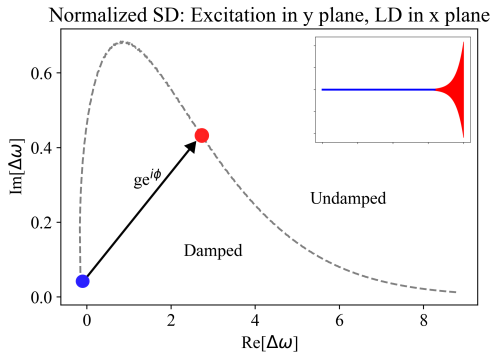

Figure 1: Normalized Stability Diagram. Excitation is fed in the y-plane and nonlinear focusing is fed in the x-plane.

position, with increasing G for one determined ϕ. The blue line represents the beam centroid position when G is too small to incite an instability and the red region represents the beam centroid position when the G and ϕ combination make $\Delta\omega$ large enough to generate an instability with growth rate g, right when the first excitation growth is observed. This threshold g and ϕ are used in Eq. (3) to map onto the SD, at the red dot in Fig. 1. Therefore, increasing G at every ϕ until the first instability results a full mapping of the SD.

A proof-of-principle experiment of this method was performed at CERN [3], where the IOTA experiment aims to quantify the capabilities of this method and obtain the beam distribution function directly from the SD, which has not been done before and would supply a new method to directly measure distribution tails [2].

METHODS

To create an antidamper, the polarity of a transverse feedback is reversed to provide the coherent excitation. The main experimental elements include a stripline kicker, two stripline BPMs, and a string of octupoles. The kicker and BPMs form the antidamper. The kicker changes the excitation gain and the two BPMs combine to create a virtual bpm, providing phase adjustment. The octupoles supply the LD [4]. There are nine octupoles in IOTA, as shown in Fig. 2, along with the other experimental elements. All the octupoles were set to the same current of 4A, large enough to dominate nonlinear focusing in the ring.

To obtain each point on the SD, the phase, ϕ, was set via setting the BPM coefficients, and the kicker gain was swept through from low gain to high gain. After calibrating between gain and growth rate, the first gain per phase with an instability gave the threshold growth rate, g. The threshold growth rate and phase were therefore experimentally obtained and used in Eq. (3) to map out the SD.

EXPERIMENTAL RESULTS

In order to analyze the experimental results, the phase advance ϕ was first obtained by converting the BPM coefficients into ϕ by performing a Beam Transfer Function

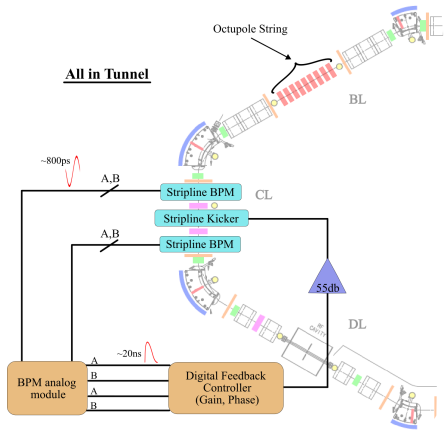

Figure 2: Schematic of experimental setup at IOTA.

(BTF) of the lower and upper sidebands per BPM coefficient pair. The BTF excited the beam, giving a frequency dependence of the beam response, where phases with the maximum beam responses were used in calculating the total phase advance from virtual pickup to kicker. Since the BTF range did not cover the full phase map, data was taken at different additional turns in the ring, allowing for data at more phases on the Stability Diagram. The data presented here corresponds to two turns prior to data collection.

To obtain the threshold growth rate per phase, we determined the knee in the gain vs. growth rate relationship. A simulated example of the gain vs. growth rate relationship is shown in Fig.4. We then used Eq. (3) to obtain Re[$\Delta\omega$] and Im[$\Delta\omega$] for the SD. The SD for the two additional turn data can be seen in Fig. 3.

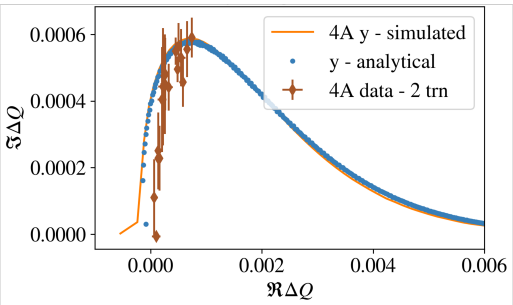

Figure 3: Experimental SD.

As can be seen, there are large uncertainties and a systematic rightward shift of the data. The error bar sources are mainly from the BTF step size and gain sweep step size. In studying the simulations and preparing for the next run of data collection, we aim to investigate these issues.

SIMULATIONS

Simulations are being used to confirm the experimental procedure, compare with theoretical predictions, and develop the method to obtain the distribution function from

ISBN: 978-3-95450-261-5 ISSN: 2673-7000 doi: 10.18429/JACoW-NAPAC2025-TUP053

the SD. The codes being used for these simulations are the simulation code PyHeadTail [5] and the package Xsuite [6].

In confirming and clarifying the experimental procedure, we first aimed to clarify the identification of the knee in the growth rate vs. gain relationship by exploring various fitting methods and gain sweep step sizes. An example of the resulting simulated growth rate versus gain at a particular ϕ is shown in Fig. 4. The threshold gain can be seen at the knee, which is calibrated to correspond to threshold growth rate.

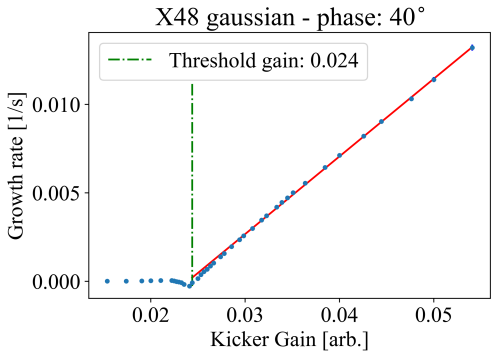

Figure 4: Example of simulated gain vs. growth rate result at $\phi = 40°$. The threshold occurs at the knee.

By obtaining the growth rate knee for other phases between $90° - 0°$, we obtain the simulated SD. The resulting simulated SD for a gaussian beam, along with the predicted Xsuite and analytical SDs are shown in Fig. 5.

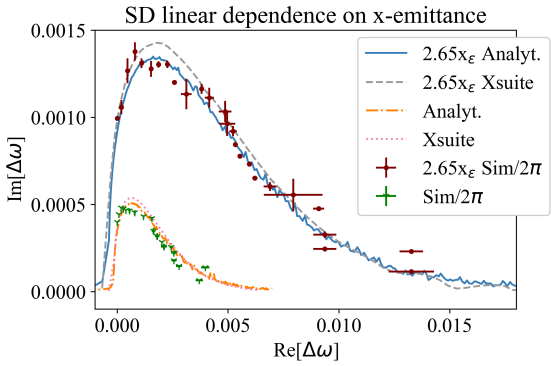

Figure 5: Simulated SDs compared with expected. SD scales linearly with x-emittance. The 2π factor is for normalization.

As can be seen, the simulated results agree with the analytical and Xsuite predictions. The size of the simulated stability diagram scales linearly with the beam emittance and nonlinearity coefficient, as predicted in Eq. (4). An example of the emittance scaling is shown in Fig. 5, where the larger SD has an x-emittance 2.65 times larger than that of the smaller SD. The size difference between these SD's is indeed ~2.65.

To approach the inverse stability problem, the SD can be used to obtain the tails of the beam distribution function, in the limit of J_x' where $\int_{J_x'}^{\infty} F_x(J_x) << 1$. Following the procedure in [2], the approximation for the beam distribution function at the tails is as follows:

$$F_x(J_x) \approx \frac{\mathrm{Im}[\Delta\omega]}{\pi \mathrm{Re}[\Delta\omega]^2} k\epsilon \tag{5}$$

Therefore, the beam distribution function at the tails can be obtained directly from the axes of the stability diagram. Doing this for the $2.65\,x_\epsilon$ gaussian SD, we get the simulated points in Fig. 6. As can be seen, the simulated beam distribution aligns well with the expected distribution at the tails. The next step is to obtain the core of the distribution function, as outlined in [2] .

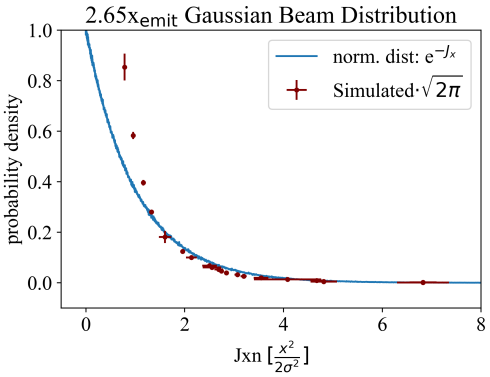

Figure 6: Inverse Stability Problem beam distribution function compared with input gaussian beam distribution. The $\sqrt{2\pi}$ factor is for normalization.

CONCLUSIONS AND NEXT STEPS

The successes of the previous run at IOTA include an increase in the number of phase measurements and many insights gained for upcoming experimental runs.

Next steps for this experiment include investigating the systematic rightward shift in our data and further investigating questions from data collection. Next steps also include performing simulations to obtain the core of the beam distribution function from the SD [2] and simulating the process of obtaining the beam distribution function for distributions other than gaussian.

Goals for the next run include taking SD data for various octupole settings, obtaining data at the SD tails, taking tighter BTF measurements, and directly measuring the amplitude detuning matrix.

ACKNOWLEDGEMENTS

We would like to thank the teams at the University of Chicago, Fermilab, and the IOTA/FAST collaboration for their support. We would also like to thank Alexey Burov for the many helpful discussions. This research is funded by the Tigner Traineeship through the Center for Bright

ISBN: 978-3-95450-261-5 ISSN: 2673-7000 doi: 10.18429/JACoW-NAPAC2025-TUP053

Beams (CBB). This manuscript has been authored by FermiForward Discovery Group, LLC under Contract No. 89243024CSC000002 with the U.S. Department of Energy, Office of Science, Office of High Energy Physics.

REFERENCES

[1] L. Palumbo and M. Migliorati, "Landau damping in particle accelerators", SAPIENZA University, Rome, Italy and INFN-LNF, unpublished, Sept. 2011.

[2] A. Burov, "Inverse stability problem in beam dynamics", *Phys. Rev. Accel. Beams*, vol. 26, p. 082801, Aug. 2023. doi:10.1103/PhysRevAccelBeams.26.082801

[3] S. Antipov *et al.*, "Proof-of-principle direct measurement of landau damping strength at the large hadron collider with an antidamper", *Phy. Rev. Lett.*, vol. 126, p. 164801, Apr. 2021. doi:10.1103/PhysRevLett.126.164801

[4] N. Eddy *et al.*, "Iota experiment nonlinear optics: Landau damping (niold)", Fermilab IOTA/FAST Experiment Proposal, unpublished, Apr. 2022.

[5] A. Oeftiger, "An overview of pyheadtail", CERN Accelerator Note, Apr. 2019. doi:10.17181/CERN-ACC-NOTE-2019-0013

[6] G. Iadarola *et al.*, "Xsuite: An integrated beam physics simulation framework", 2023. doi:10.18429/JACoW-HB2023-TUA2I1